

# Stochastic description of sea waves

## Description stochastique des vagues de mer

CONSTANTINE MEMOS, *Associate Professor, School of Civil Engineering, National Technical University of Athens, Heroon Polytechniou 5, 157 80 Zografos, Greece*

with contributions by K. TZANIS and K. ZOGRAPHOU, *Postgraduate students.*

### ABSTRACT

An alternative to spectral description of sea waves in water of any depth is proposed based on the stochastic nature of the sea surface. The suggested short-term representation of a sea state displays a probabilistic structure in terms of joint densities of wave heights and periods that is advantageous in the design of maritime structures. Models have been developed and supported by laboratory and field data studies that are capable of providing the said stochastic description in a manageable form and with acceptable accuracy. Lines of further research are described for investigating this relatively unexplored field in maritime hydraulics.

### RÉSUMÉ

On propose une alternative à la description spectrale des vagues de mer à une profondeur quelconque qui se base sur la nature stochastique de la surface de la mer. La représentation à court-terme d'un état de la mer suggérée comprend une structure probabiliste aux termes de densités combinées des hauteurs des vagues et des périodes, ce qui est avantageux pour la dimensionnement des structures maritimes. Des modèles numériques ont été développés et soutenus par des données du laboratoire et du terrain. Ces modèles sont capables de fournir la description stochastique ci-dessus à une forme maniable et avec une précision acceptable. Des lignes de recherche plus ample sont proposées afin d'explorer ce domaine d'hydraulique maritime qui est relativement inexploré.

### 1 Introductory Overview

Stochastic processes can be regarded as providing a closer approximation to reality, rather than a human invention to accommodate our deficiency in understanding the physical world. A real-life problem cannot be completely described by any infinite number of parameters, thus it cannot be fully represented in a deterministic way. The stochastic representation of a system should not be considered, however, as a rival to determinism, but rather as a higher level of approximation to reality than the relevant deterministic laws governing the physical processes in the elements of the system.

Sea waves are a good example of a stochastic process that can be expressed in terms of one or more random variables, such as the elevation of the free surface at a fixed point, the surface slope, or other characteristic parameter. The stochastic description of the sea surface was greatly based on the remarkable progress achieved during the past century in the area of spectral analysis of random variables. Indeed, the representation of surface wind-driven waves in terms of power spectral density (i.e. mechanical energy per frequency component) characterising a certain sea state has been extensively used in models of wave generation and propagation in both offshore and coastal areas. Spectral transformation models (e.g. WAMDI group [26], Holthuijsen et al. [8]) are nowadays routinely used in wave prediction. Another class of wave transformation models is based on time series realizations of the free surface yielded by the said spectral representation of a sea state (e.g. Ishii et al. [9], Nwogu and Mansard [21]). The advantage of the more detailed description of the wave field afforded by these time-domain models is offset by their demanding computing requirements. These requirements limit at present their

field of application to areas a few kilometers across, while spectral models can be applied satisfactorily to vast ocean regions.

An alternative to the above representations is the short-term probabilistic description of a sea state, dealt with in this article. This description is based on crucial, from an engineering point of view, characteristics of the wave field, namely on the random variables "wave height  $H$ " and "wave period  $T$ ". A stochastic representation of the short-term probabilistic structure of the wave field, involving the joint probability between wave heights and periods would be advantageous in the design of maritime structures, by enabling probabilistic approaches, including risk analysis. Such a probabilistic representation of a sea state displays explicitly the information pertaining to the joint occurrence of wave heights and periods, in contrast to spectral representation. This information is now widely accepted as a prerequisite for a more accurate estimate of random wave loading on maritime structures. The conventional practice of calculating wave forces on fixed structures by using only the wave height could well be regarded as quite crude in the near future.

The basic design of breakwaters can be based on the values of the  $(H,T)$  pairs along with their associated probability of occurrence through refined techniques, of probabilistic or deterministic character (e.g. Van der Meer [25], Losada et al. [14]). Other aspects of the design of such structures can also benefit from this information, e.g. the accurate estimation of overtopping and consequently of the crown elevation of coastal structures. Time-dependent processes that relate to design considerations can also be better described through the use of the triads  $(H,T,p)$ , where  $p$  is probability density, facilitating improved design. Such processes might include undertoe scouring, the dynamic stability of non-armoured breakwaters, the displacement of armour units in con-

Revision received April 17, 2002. Open for discussion till October 31, 2002.

ventional or berm-breakwaters, etc.

Since a lot of research and relevant results are based on the spectral description of sea waves, it would be desirable this description to be linked to the probabilistic representation under consideration. However, establishing an one-to-one relation between the power spectrum and its corresponding probabilistic structure and vice versa, cannot apparently be achieved in a simple way. This can be attributed to the fact that real-life wave spectra cannot be defined through a single parameter, whereas the probabilistic description can virtually, at least for deep water waves, as will be seen later.

Results of some research efforts support the above. Indeed, attempts have been made to correlate the two representations, spectral and probabilistic, through key parameters. The parameters chosen are associated to the presence of waves of different periods in the sea state under consideration. They include the spectral width parameter  $\epsilon$  for the spectral, and the correlation coefficient  $r(H,T)$  for the probabilistic description. An alternative to  $\epsilon$  was also studied, namely the bandwidth parameter  $\nu$  introduced by Longuet-Higgins [11]. These three parameters are defined as:

$$\epsilon = (1 - m_2^2/m_0 m_4)^{1/2} \quad (1)$$

$$\nu = (m_0 m_2 / m_1^2 - 1)^{1/2} \quad (2)$$

$$r(H,T) = \sum_{N_0} (H_i - H_m)(T_i - T_m) / \sigma_H \sigma_T N_0 \quad (3)$$

where,  $m_i = \int_0^\infty \omega^i S(\omega) d\omega$ ,  $S(\omega)$  the power spectrum,  $\omega$  the circular

frequency,  $\sigma_H$ ,  $\sigma_T$  the standard deviation of the wave height, period respectively, and subscript  $m$  denotes mean value.

Numerical experiments by Goda [6] and some limited results by Memos & Tzanis [18] suggest a weak qualitative relationship between  $\epsilon$  and  $r$ . The results of a more thorough investigation (see section 2) only supports a general trend between  $\epsilon$  and  $r$ , and slightly better between  $\nu$  and  $r$  in deep water. As can be seen from Fig. 1, experimental data from 84 records in 14 tests in shallow water taken at HR Wallingford (section 2), indicate little support for a relationship of any kind. Thus, the initial conjecture that an

$\epsilon$ - $r$  (or  $\nu$ - $r$ ) relationship may not be feasible, seems to be supported by experimental measurements.

Referring to wave propagation models in coastal waters a way to proceed with the probabilistic representation, given, as previously described, that a link with the spectral description is not easily established, would be to perform wave-by-wave analysis of the joint H-T probability density of the incoming waves and combine the results at the point of interest. This approach often disregards the interactions between individual wave components but, nevertheless, is quite powerful for engineering applications. An effort was made along these lines by addressing a case with long-crested random waves at normal incidence to the coastline. The effects of shoaling, wave breaking, and wave reforming were taken into account. The results of such a synthetic model when compared to experimental measurements were very encouraging as shown in section 4.2.

Wave directionality is an important factor in many applications, despite the fact that in coastal regions wave direction varies within a more or less narrow band, depending on refraction effects. The joint H-T density dealt with in this article is made up by waves of all directions at a fixed point. This is in accordance to the basic assumptions pertaining to the properties of free surface elevation. It is possible, under widely accepted assumptions on energy spread, to display directionality in the probabilistic description of a sea state in deep water.

In a wave-by-wave analysis the refraction effects need also be incorporated. In such a set-up, one could start from deep water with known input in the form of probabilistic description including directionality and transform the individual waves inshore taking into account the main processes present in each case. This does not preclude, in principle, allowing for wave-wave interactions, although this would require a vast amount of computations. Finally, at the points of interest the properties of the incoming waves would be summed up in a way compatible with the stochastic representation, including wave directionality. This is an area for further research mentioned in section 5. Experimental investigations are described briefly in the next section. Results regarding the stochastic imprint of sea waves in deep water are presented in section 3. In section 4 modifications for intermediate and shallow water are described.

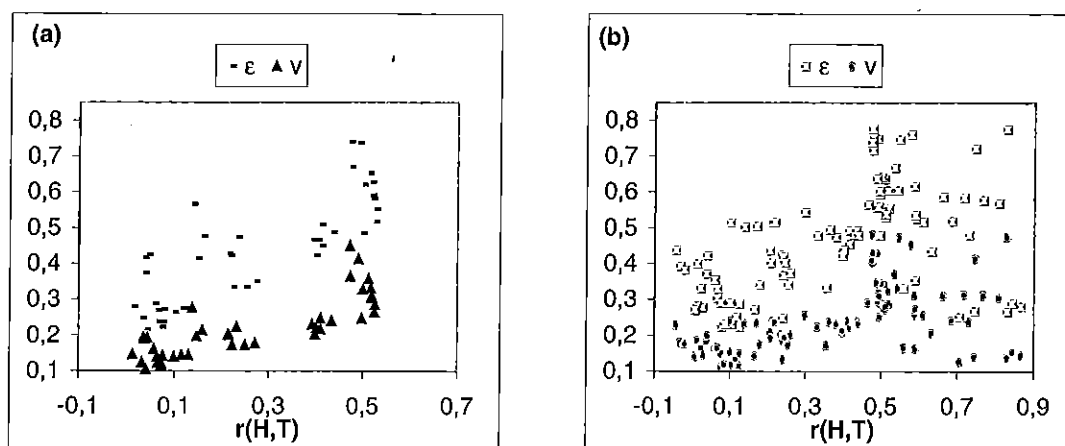


Fig. 1 Scatter diagrams  $r$ - $\epsilon$  and  $r$ - $\nu$ : (a) deep water; (b) shallow water.

## 2 Experiments at HR Wallingford

Experimental tests were conducted at the UK Coastal Research Facility at HR Wallingford during a period of 12 weeks. The experiments aimed at studying various aspects of random wave propagation in shallow water, such as evolution of the joint H-T density and its correlation with spectra, wave directionality, and particle kinematics in the surf zone. The wave basin has overall dimensions 27m x 54m and contains a narrow strip of horizontal bed and a rigid beach sloping uniformly at 5%. The wave maker consists of 72 electronically-driven wave paddles 0.50m wide that can produce random long- and short-crested waves of prescribed target spectrum and directional spread. The long-crested waves can be generated at an incidence from 0 to 30° to the shore. The facility can also produce currents parallel to the shoreline with tidal or breaking waves origin. The maximum surface current that can be produced for a 0.50m nominal water depth is 0.14 m/s. The water depth over the horizontal bed can vary from 0.30m up to 0.80m, thus accommodating a limited range of deep water conditions. The period of monochromatic waves lies within the band 0.8s to 3s. A thorough description and evaluation of this facility can be found in Simons et al. [22].

Measurements of the free surface elevation were taken electronically with capacitance-resistance probes located as shown in Fig. 2. The duration of each run ranged from 14min to 20min to sample on average about 1000 waveforms. Analysis of the time series was performed mainly through specially developed software. The wave energy absorption was effected by a gravel beach of

mild slope. The main parameters of the tests, to be used in the following, are presented in Table 1. The directional spread noted as  $\cos^2$  in this table refers to the expression of the spread function:

$$D(\theta) = \frac{2}{\pi} \cos^2 \theta, \quad -\frac{\pi}{2} < \theta < \frac{\pi}{2} \quad (4)$$

while the one noted as Mits. to the Mitsuyasu type of directional spreading function (Mitsuyasu et al. [10]).

Table 1. Main input parameters of tests.

Test	Waves	Spectrum	$T_p(s)$	$H_s(m)$	Energy Spread
R8-1	Long crested	Jonswap $\gamma=9.9$	0.8	0.04	-
R8-2	Long crested	Jonswap $\gamma=9.9$	0.8	0.07	-
R8-4	Long crested	Jonswap $\gamma=3.3$	0.8	0.04	-
R8-7	Long crested	Jonswap $\gamma=3.3$	0.8	0.04	-
R8-8	Long crested	Jonswap $\gamma=3.3$	0.8	0.07	-
R8-11	Short crested	Jonswap $\gamma=3.3$	0.8	0.07	$\cos^2$
R8-37	Short crested	Jonswap $\gamma=3.3$	1.4	0.12	Mits.
R8-38	Long crested	Jonswap $\gamma=3.3$	1.4	0.15	-
R8-39	Short crested	Jonswap $\gamma=3.3$	1.4	0.07	Mits.
R8-40	Long crested	Pierson-Mosk.	1.4	0.08	-
R8-63	Long crested	Jonswap $\gamma=7$	1.2	0.09	-
R8-67	Short crested	Jonswap $\gamma=7$	1.2	0.12	$\cos^2$
R8-76	Long crested	Jonswap $\gamma=7$	1.4	0.15	-

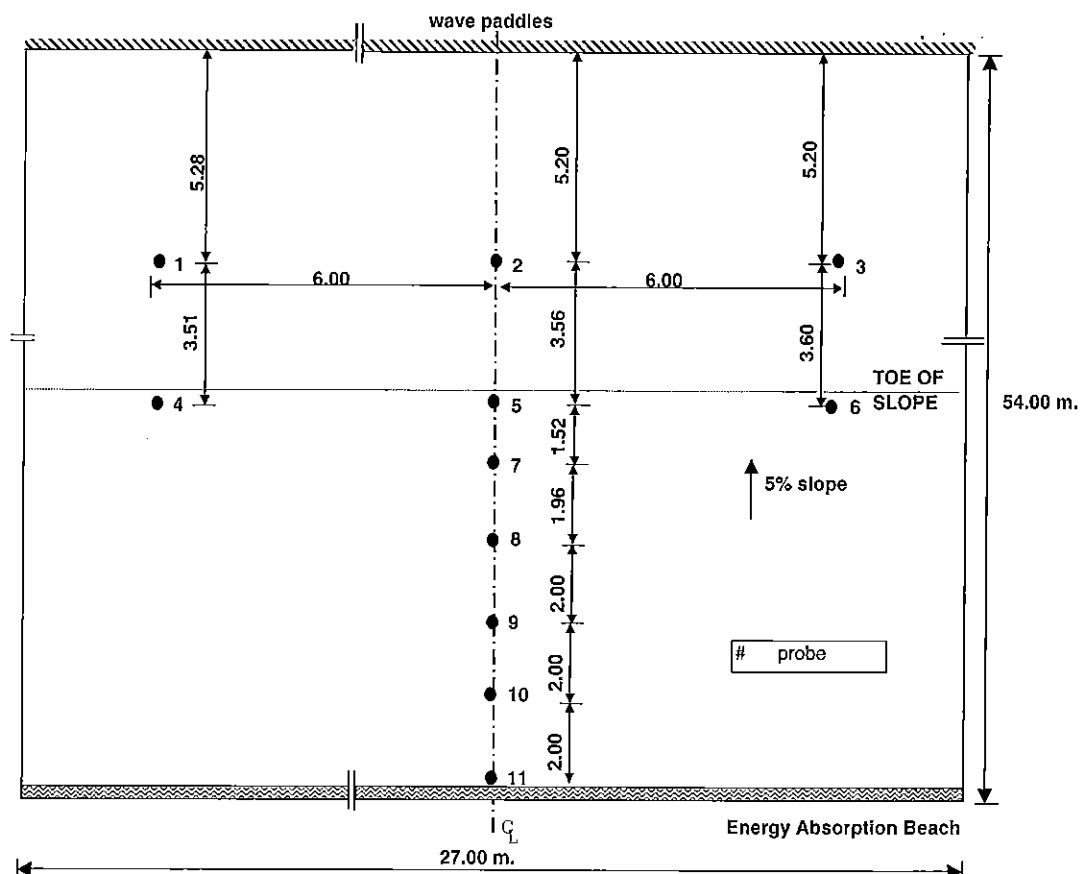


Fig. 2 Experimental layout plan.

### 3 Stochastic Imprint in Deep Water

#### 3.1 Joint probability density of $H$ - $T$

The problem of describing a sea state in a stochastic manner in terms of the joint density of wave heights and periods is quite complex. So far, only a few treatments have yielded results, which, however, are applicable mainly to narrow-banded seas in deep water (e.g. Cavanié et al. [2]; Longuet-Higgins [13]). More recently, Memos and Tzanis [18,19] developed a parametric model that provides numerical results of this joint density for deep water waves of any bandwidth.

Under the assumptions of ergodicity and normal distribution of the free surface elevation, the model provides a stochastic representation of surface waves in terms of the short-term joint probability density function between wave height and period, as measured by the zero up-crossing procedure. The input required for producing this density is minimal and can be defined with only two parameters: (a) the "magnitude" of the sea state, i.e. given by a characteristic heightwise measure, as e.g. the significant wave height  $H'_s = H_s / H_*$  normalized with respect to an accepted minimum wave height, in the record under examination, and (b) a non-dimensional parameter  $\alpha$ , defined as a mean wave steepness (i.e. the ratio of the mean wave height  $H_m$  to the mean wavelength  $L_m$ ). It is noted that the model shows a low sensitivity to variations of  $\alpha$ , mainly because it relates only two characteristic parameters of the sea without imposing any other restriction to the numerous pairs of the individual wave heights and wavelengths. The input parameter  $H'_s$  can be substituted by any other similar quantity, such as the normalized mean wave height  $H'_m = H_m / H_*$ . The heightwise resolution of the grid assumed in the present model plays a role in defining the model value of  $H_*$ . This value has to be assumed in any analysis of a real record, leading to a similar assumption as to the high cut-off frequency of the relevant power spectrum.

The results presented in this paper are based on a  $2 \times 20$  heightwise grid that allows for a range of possible wave heights, where the ratio of maximum to minimum wave height within a sea state could be up to 20, which is plausible assumption. This range is not necessarily covered entirely in all cases, especially for small values of  $H'_s$ . Evidently, the behaviour of  $H'_s$  is monotonically linked with the non-dimensional standard deviation  $\sigma'_\eta = \sigma_\eta / H_*$  of the free surface elevation. It is further noted that the results presented here were obtained on the assumption  $\eta_{\max} + \eta_{\min} \geq 0$  for each particular wave in the record.

The above input data can be estimated in real life situations by employing conventional wave forecasting techniques. Deep water wave breaking is taken into account, and separation of swell from wind waves can also be accommodated by the model. Panels 3a,b,c present examples of probabilistic representations of sea states in deep water for various  $\sigma'_\eta$  with  $\alpha=0.05$ . In these graphs a deep-water wave breaking criterion of  $\alpha=0.143$  has been imposed. The cut-off period adopted required  $T_{\max} < 2.5T_m$ , where the subscript m indicates mean value. For the sake of comparison corresponding graphs of field measurements have been included in the same figure, as well as experimental results from one of the tests of Table 1.

The experimental result in Fig. 3d refers to deep water conditions of test R8-38 (Table 1) with  $r(H,T)=0.42$ . Field measurements from North Atlantic (Goda [6]), and the Mediterranean (National Centre for Marine Research, Greece) provided the graphs of panels 3e and 3f, respectively. These graphs were selected for their being associated with high values of correlation coefficient  $r(H,T)$ , so that they can be compared with model results presented in Fig. 3b,c.

It can be seen from Fig.3 that the layout of the model graphs is favourably compared with experimental and field measurements at both medium and high  $r$ -values. A characteristic property of these joint density graphs relates to the inclination in the  $H$ - $T$  plane of the "ridge" curve of minimum slope in the  $(H,T;p)$  space, for values  $H > H_m$ , marked by the broken line on the graphs of Fig.

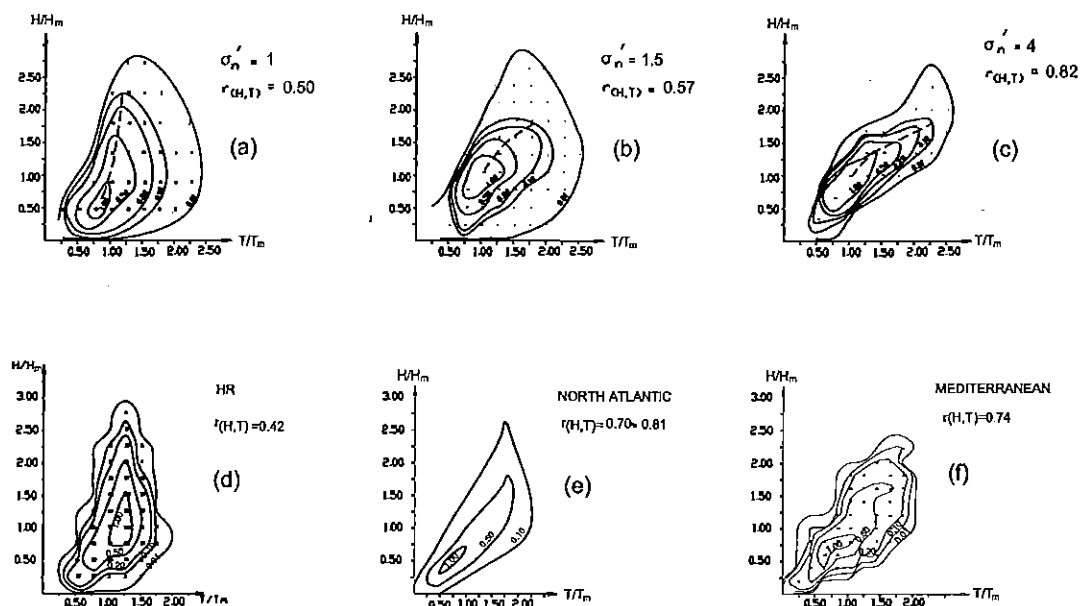


Fig. 3 Probabilistic representations in deep water. Model: (a), (b), (c); Experiment (d); Field data: (e), (f).

3a,b,c. If this curve tends to be perpendicular to the T-axis then a symmetry of the graph in this range of wave heights develops and the H-T correlation becomes insignificant. In contrast, when the above curve tends to be inclined to the T-axis, then it is evident that the H-T correlation for large H becomes stronger. This expected property of the joint H-T density is satisfactorily reproduced by the model under consideration as can be seen in Fig. 3. Indeed, for increasing  $r(H, T)$ , the said "ridge" curve tends to incline toward the T-axis. This is a comforting result since it suggests that the inner structure of the model is physically sound. The numerical experiments confirmed that any sea state associated with a given  $H'_s$  or  $\sigma'_\eta$  is directly related to a value of the correlation coefficient  $r(H, T)$ . The following table gives some characteristic values of the above quantities resulted from these tests.

Table 2. Characteristic statistical values

$\sigma'_\eta$ (input)	$H'_s$	$H'_m$	$r(H, T)$
1.5	5.31	3.76	0.57
2	7.25	4.98	0.69
3	10.15	7.07	0.80
4	12.69	8.83	0.82

The numerical tests performed show a monotonic correlation between  $H'_s$ ,  $\sigma'_\eta$ , and  $r(H, T)$ , meaning that for larger wave heights the correlation between H and T becomes stronger. This is indeed reflected in the diagrams presented in Fig. 3. For increasing  $H'_s$  the density masses tend to accumulate close to the "ridge" curve in the joint density graphs, suggesting a higher correlation coefficient. The maximum value of  $r(H, T)$  (close to 0.85) reached during the numerical experiments represents an upper limit of the correlation coefficient also observed in nature (Goda [6]).

A similar feature emerging from the numerical results refers to the invariability of the stochastic signature of a sea state for large values of  $\sigma'_\eta$  or  $H'$ . It was found that for  $\sigma'_\eta$  higher than about 2.5, no significant modifications to the stochastic description of the sea state are incurred.

### 3.2 Probability density of H

A useful by-product of the description presented in the previous section is that the marginal probability density of wave heights can be obtained from the corresponding joint density. It is quite

interesting to compare the results of this model for deep water with the Rayleigh distribution, commonly used to describe the density of wave heights. This distribution refers to a narrow-banded power spectrum of the sea state, however. In Fig. 4 density curves are presented of the quantity  $H/H_m$  for two values of  $r(H, T)$ . These are related, according to the previous discussion, to corresponding values of  $H'_s$ , or equivalently of the standard deviation of the surface elevation  $\sigma'_\eta$ . Both graphs of Fig. 4 include also results of buoy measurements taken in the Mediterranean by the National Centre for Marine Research, Greece. Panel (a) corresponds to  $r(H, T)=0.5$ , and panel (b) to  $r(H, T)=0.7$  for both model and field data.

These graphs, and others not presented here, show that as  $H'_s$  or  $\sigma'_\eta$  increases, the density of  $H/H_m$  around the peak increases also, deviating from the Rayleigh peak density to an upper bound curve. The model suggests a maximum density of about  $p(H/H_m)=1.1$  occurring at a value of H close to  $0.9 H_m$ . The above trend suggests that when no restrictions to the "bandwidth" of the sea state are imposed, then, in the framework of this model, the Rayleigh distribution is associated with a very small variance of the surface elevation. In other words, the higher the wave height, the larger the deviation from the Rayleigh density in a wide-banded sea.

### 3.3 Probability density of T

The joint density referred to previously (section 3.1) can also provide a picture of the stochastic structure of the wave period in deep water. The corresponding marginal density of  $T/T_m$  is depicted in Fig. 5 for four different sea states characterized by their associated representative  $\sigma'_\eta$  (see Table 2).

As noted previously (section 3.2), the density curves tend to a "saturation" level for values of  $\sigma'_\eta$  higher than about 2.0, i.e. for most broad-banded sea states. For these values of  $\sigma'_\eta$  the probability density function of  $T/T_m$  remains insensitive to the actual value of  $\sigma'_\eta$ . In a Rayleigh distribution, i.e. in a narrow-banded sea, the value of the ratio  $H_m/\sigma_\eta$  is 2.51. The present model suggests that in a broad-banded sea state, this ratio can go down to about 2.1 in a very wide-banded sea (cf. Table 2). The maximum density of the normalized period occurs around  $p(T/T_m)=1.2$  for  $T=T_m$ , where  $T_m$  is the mean period.

### 3.4 Summary

In summary, the offshore joint probability density of wave

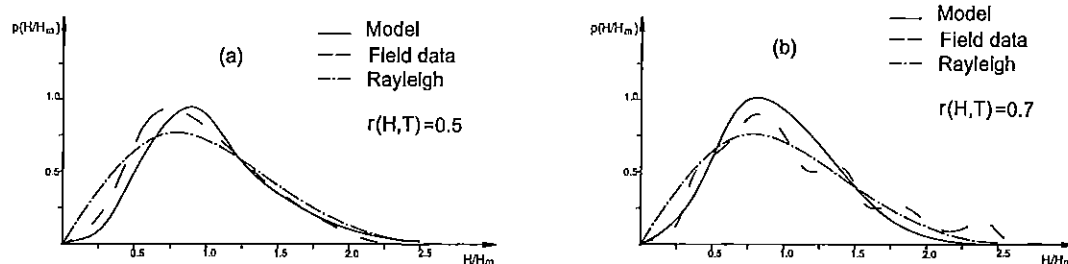


Fig. 4 Density of wave height in deep water: (a)  $r(H, T)=0.5$ ; (b)  $r(H, T)=0.7$

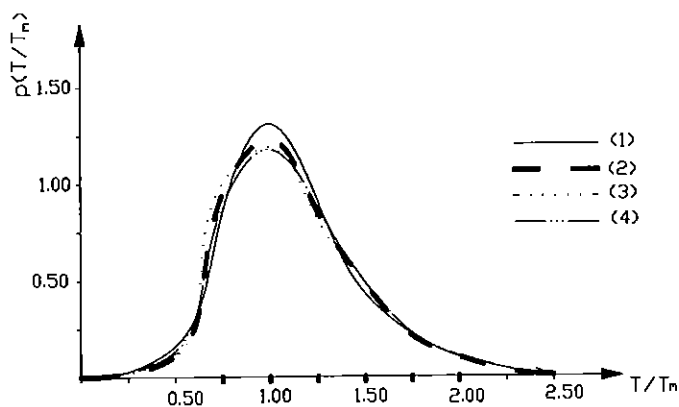


Fig. 5 Density of wave period in deep water: (1)  $\sigma'_\eta = 1.5$ ; (2)  $\sigma'_\eta = 2.0$ ; (3)  $\sigma'_\eta = 3.0$ ; (4)  $\sigma'_\eta = 4.0$

heights and periods can be obtained through the following main steps:

1. Definition of the desired input value of  $\sigma'_\eta$  according to the severity of the sea state to be studied.
2. Generation of a model record, by waveforms of arbitrary wavelength and randomly produced realizations of these waveforms.
3. Estimation of the period associated with each individual waveform of the model record through a stochastic process technique.
4. Exclusion of swell, if required, through a  $T/T_m < M$  criterion, where  $M$  a suitable number, say  $M=2.5$ .
5. Application of deep water wave breaking filtering.
6. Production of the joint density graph from the processed record for any required values of  $H'_i$  and  $\alpha$ .
7. Calculation of the corresponding value  $r(H, T)$ .

The wave-generating code produced some 50,000 waveforms, which were then treated using the statistical theory of random processes. Details on the development of the stochastic model that produces the joint density  $p(H, T)$  can be found in Memos and Tzanis [18,19] where additional references are also provided.

Results of the deep water model for the short-term joint probability density of wave heights and periods are encouraging, properly displaying the contraction and the inclination of the "ridge" of the iso-density contours along a narrower zone as  $r$  increases, a fact not reproduced by past approaches.

## 4 Shallow Water Modifications

### 4.1 Background

Most maritime civil engineering works are built within the coastal zone. Knowledge of the behaviour of the wave field in shallow water is, therefore, of paramount importance from an engineering point of view. Compared with waves in deep water, waves in coastal areas are much more complex to model. In addition to factors that influence wave propagation in deep waters (such as wind action, dissipation due to "white capping", non-linear interactions), shallow water waves are substantially affected by processes such as shoaling, refraction, wave breaking, wave reform-

ing, and bottom friction. The combined effect of all these processes is extremely complex to predict. Models have been developed, however, that can take into account a number of the above factors.

As mentioned in section 1 one way to overcome the difficulty of coupling the probabilistic description with spectral inshore models is to apply a wave-by-wave treatment on a known joint density in deep water. It has been shown (e.g. Mase and Kobayashi [16], Dally [4]) that in shallow water the statistical behaviour of the wave field can be predicted within acceptable limits by a wave-by-wave analysis of the incoming waves. The individual results can be combined in an appropriate way to construct the corresponding joint density at any point in shallow water. This approach has been pursued (Memos [17], Memos & Tzanis [19]) in a relatively simple situation when no wave refraction is present. The other main processes present in coastal waters (i.e. wave shoaling, depth induced wave breaking and wave reforming after breaking) have all been taken into account in this synthetic wave transformation model.

Stokes and cnoidal wave theories have been used in the description of shoaling waves. Both theories produce waves of permanent form and, thus, cannot represent adequately the evolution of a wavetrain propagating into shallow waters, where skewness of the wave form is increasingly being developed. However, it should be remembered that the use of these theories in the present context aims at predicting the probabilistic structure of the wave regime at any inshore location. This regime can be represented by the associated structure of a few main wave characteristics, e.g. wave heights and periods. These parameters are not seriously affected by the detailed geometry of the free surface, as shown by Goda [7] and Stansberg [23], who concluded that wave height distribution is not affected by the degree of wave asymmetry, or by the statistical skewness of the surface elevation record.

The model takes into account third-order Stokes waves undergoing nonlinear shoaling in the zone where  $d/L < 1/8$  and  $Ur > 26$  (for details see Memos & Tzanis [19]). Shoreward of this zone cnoidal shoaling was applied. The local values of wave characteristics determined by the above procedure are checked for depth-induced wave breaking through a relevant frequency-dependant criterion (Weggel [27]). Finally, wave decay and reforming after breaking have been incorporated in the model following a proposal by Dally et al. [3]. It is further assumed that the individual waves retain their associated periods throughout the shoaling process up to the breaking point.

Transformations of wave characteristics across a uniformly sloping beach have been investigated in various experimental studies. The modifications upon the stochastic imprint of the sea state represented by a joint H-T density have been studied in experiments described, among others, in Memos [17], Memos & Tzanis [19] and below in this paper.

### 4.2 Transformation of the Stochastic Imprint

This synthetic model can provide stochastic representations in the nearshore, when refraction and higher order interactions can be neglected. A couple of graphs at different water depths for a par-

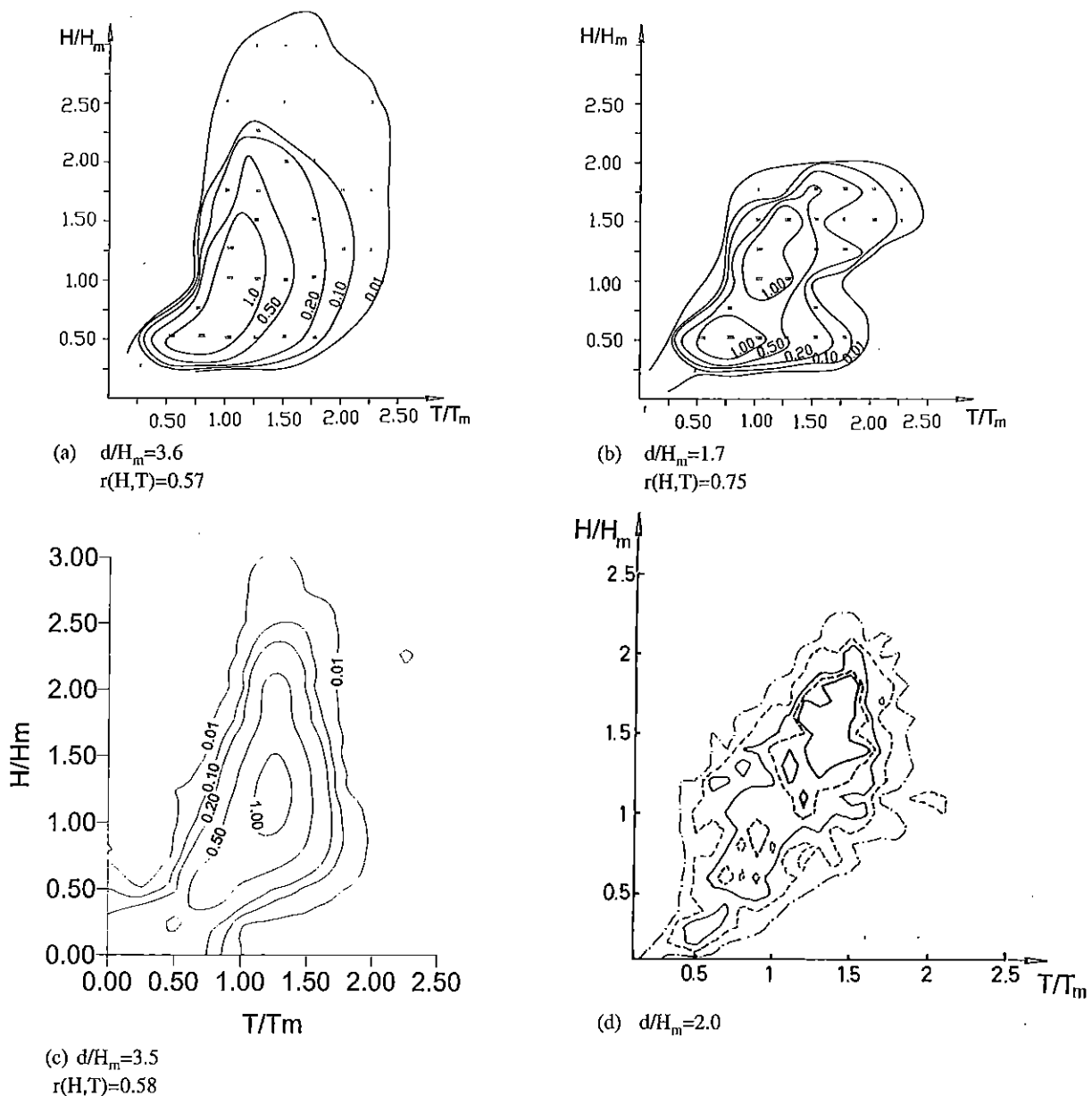


Fig. 6 Joint H-T density in shallow water for 5% slope. Model: (a), (b); Experiments: (c) HR, (d) Doering and Donelan

ticular offshore sea state are given in Fig. 6a, b. Results are also included from artificial sea states of similar characteristics produced during laboratory experiments. Graph 6c was obtained from test R8-38 with  $d/H_m=3.5$  and  $r(H,T)=0.58$ , to be compared with model results of panel 6a; panel (d), reproduced from Doering and Donelan [5], refers to an experimental set-up with  $d/H_m=2.0$ , thus it should be compared with panel 6b. It is noted that graph 6d gives the density as a ratio to its maximum value. This, however, produces only minor differences from the way the other diagrams of Fig.6 are drawn. It can be said that, in general, the model diagrams are well supported by the experimental results, at least qualitatively.

An important feature of the shallow water model is that the results can be expressed in terms of the relative water depth defined as  $d/H_m$ . This allows the unique representation of the joint density under no-refraction conditions given the local depth, the bed slope and the corresponding offshore joint density. Variations of

the bed slope can be incorporated in the model, by assuming piecewise uniform sections.

The joint H-T density transforms by accumulating mass towards the "ridge" line as the waves travel inshore. This suggests an increased correlation between wave heights and periods as the waves propagate shoreward. Such a trend has been observed in shoaling experiments (Memos [17]) and will be discussed below. Another feature of the transformation in the stochastic structure of shoaling waves is the distinct decrease in the spread of the wave height around its mean value. Also, an increasing curvature of the "ridge" line of the  $p(H,T)$  graph as the waves propagate into shallower water is observed (Fig. 6b).

#### 4.3 Correlation between H and T

A comprehensive measure of the statistical relation between wave heights and periods is the correlation coefficient  $r(H,T)$ . The

behaviour of this coefficient as the waves move inshore has been studied, e.g. in Memos [17] and in Memos & Tzanis [19]. The conclusion of these studies is that, in general,  $r(H,T)$  tends to increase as waves travel inshore, becoming more pronounced for diminishing water depths. Shoreward of a zone of severe breaking, where most of the individual waves break and wave reforming takes place, the value of  $r(H,T)$  was found to diminish sharply. It also appears that the actual value of the bed slope does not play a significant role in the variation of  $r(H,T)$  with depth, up to a point well into the surf zone. Inshore of this point the modification of  $r(H,T)$  does depend on the sea-bed slope. Fig. 7 gives experimental measurements from 11 tests carried out at the UK Coastal Research Facility (see section 2). No clear modification pattern can be detected by inspecting results from each individual test. However, it can be said that generally  $r(H,T)$  increases with diminishing water depth. This tendency is supported by numerical experiments carried out by the present model for depths down to the breaker zone.

The above discussion refers to steady state conditions with a more or less constant value of  $r(H,T)$  at every point. This situation which in nature normally lasts a few hours, has been coined a "sea state" in the present context.

#### 4.4 Behaviour of the Wave Height

As stated earlier (section 3.2) an important by-product of the study of the joint H-T density is the behaviour of the marginal distribution giving the density of the wave height as the waves propagate into shallow waters. The term "wave height" is used as a representative measure of the corresponding stochastic variable. It is known that as waves move inshore their height distribution deviates more and more from the Rayleigh curve. During some experiments a limited redistribution of energy around the peak of the density curve has been observed (Thornton and Guza [24], Memos [17]).

The shallow water model correctly reproduces the variation of wave heights in waver trains normally incident on a uniform beach. This can be verified by comparisons to experimental data

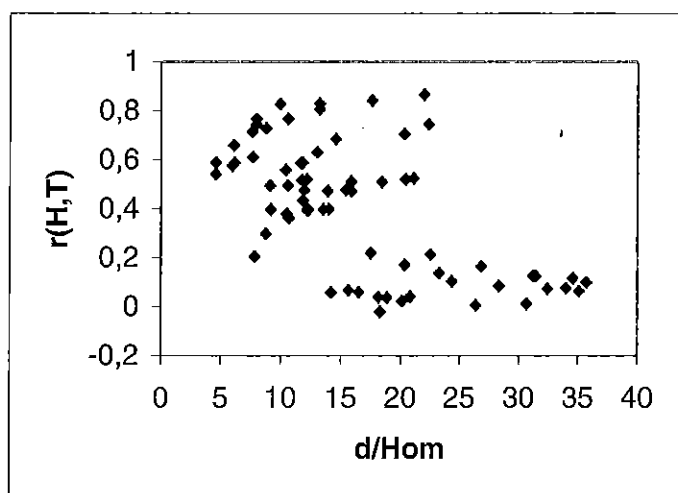
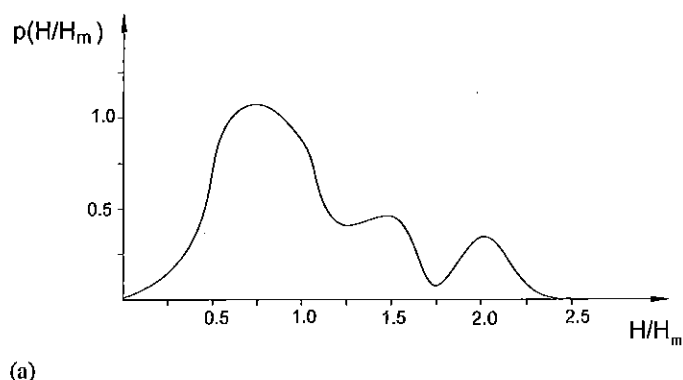


Fig. 7 Modification of  $r(H,T)$  with depth for experimental data;  $H_{om}$  is mean deep water wave height

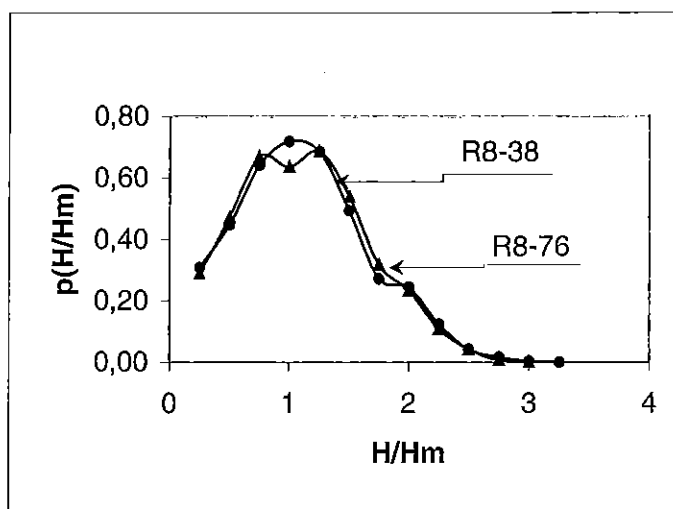
of Mase [15] and Kamphuis [10] (see Memos and Tzanis [19]). By taking a marginal density of the joint H-T density produced by the model, the H-density can be obtained as shown in Fig. 8 for  $d/H_m=3$  and bed slope 1:20. Experimental results (Table 1, tests R8-38, R8-76) with a value of  $d/H_m$  comparable to the previous one and for the same bed slope are also shown. Note that the corresponding  $p(H,T)$  graphs in deep and shallow water of test R8-38 are given in Figs 3d and 6c respectively. A deviation is noted between predicted and measured  $p(H/H_m)$ , in particular at its maximum value. This discrepancy may be attributed to the fact that the experimental results do not necessarily represent a fully arisen sea, in contrast with the model results where every wave component is represented to its full potential. This can be confirmed by the actual distribution of the surface elevation at the deep water probes, that deviated from the Gaussian and consequently from the central assumption on which the model is based.

#### 4.5 Behaviour of the Wave Period

It is important to check the approximation frequently used in practice, that the wave period remains invariant as waves propagate inshore. During experiments (Memos [17]), a mild increase of the mean period measured by the zero up-crossing method, has been observed as waves propagate into shallow water. As regards



(a)



(b)

Fig. 8 Density of wave height in shallow water ( $d/H_m=3$ ): (a) model; (b) experiments



the probability density of the wave period in shallow water the model shows essentially invariability with respect to the corresponding deep water diagram.

#### 4.6 Distribution of the Water Surface Elevation

The probability density of the excursion of the free surface around the mean is widely assumed to follow a normal distribution in deep waters. However, in shallow water this cannot be regarded as an acceptable assumption. Various proposals have been made regarding the most appropriate distribution (see e.g. Longuet-Higgins [12], Bitner [1]). Data collected during the experiments described in section 2 were processed to gain some insight in this issue for the case of normal incidence of random waves on a plane beach. The variation of both skewness,  $s$ , and kurtosis,  $k$ , of the vertical excursion was found to closely follow linear relationships with depth. The results are based on 11 tests and are presented in Fig. 9a. In this figure  $d$  denotes the local depth and  $d_0$  the deep water depth limit associated with the significant wave height of the input spectrum. To generalise the results, the straight lines of Fig. 9a have been slightly shifted so that they pass the deep water limit at the theoretical values of 0 and 3 for  $s$  and  $k$ , respectively, in the normalised Gaussian distribution. An interesting feature emerging from the above experimental results is that the rate of increase of the values of  $s$  and  $k$  with diminish-

ing depth is almost identical. The above results suggest that a parametric investigation of the surface elevation distribution in shallow water could be worthwhile.

A linear relationship was also found to apply to the first moment, mean value  $m$ , of the distribution (Fig. 9b). However, a considerable scatter is observed in the corresponding graph for the second moment (not shown). This obstacle can be overcome since the estimation of the standard deviation of the surface elevation is a parameter associated with each sea state and is, thus, readily available through the joint density algorithm. By obtaining the values of the first four moments, the searched distribution can be constructed by a Fourier transform of the corresponding characteristic function, as follows.

If the sought density is  $p(x)$  then under quite general integrability requirements:

$$p(x) = \frac{1}{2\pi} \int_{-\infty}^{\infty} e^{-itx} \varphi(t) dt \quad (5)$$

where the associated characteristic function  $\varphi(t)$  can be expressed in the following form:

$$\varphi(t) = 1 + \sum_{j=1}^{\infty} \frac{m_j}{j!} (it)^j \quad (6)$$

where  $m_j$  are the moments of the sought distribution. This topic, however, needs further investigation.

#### 5 Further Research

It is obvious that due to the little attention that the probabilistic representation of waves has attracted, there is a potential for more research and development in this area. Some of the topics that emerged during the present investigation that warrant further study are the following:

- Coupling of the present wave representation with time-domain propagation models in shallow water. This would include the task to retrieve the probabilistic image from the output of the propagation model at a given point.
- A parallel path to the previous procedure is to enrich the synthetic model referred to in section 4.1 with the refraction process. Although the model is based on theories of permanent waveforms, it is evident that it closely describes the stochastic characteristics of waves propagating inshore.
- Inclusion of wave directionality in the stochastic description of sea waves as they move from deep to shallow water will enhance the thoroughness of the approach as it will explicitly display information on wave direction. This line of research will be partially covered in the previous point through application of the refraction process.
- The non-Gaussian distribution of surface elevation in shallow waters can be further investigated through the resulting probabilistic description of waves there. Alternatively, a predetermined theoretical distribution, say a 3-parameter  $\gamma$ -distribution, can be suitably scaled to fit a set of distribution moments known a-priori (refer to section 4.6).

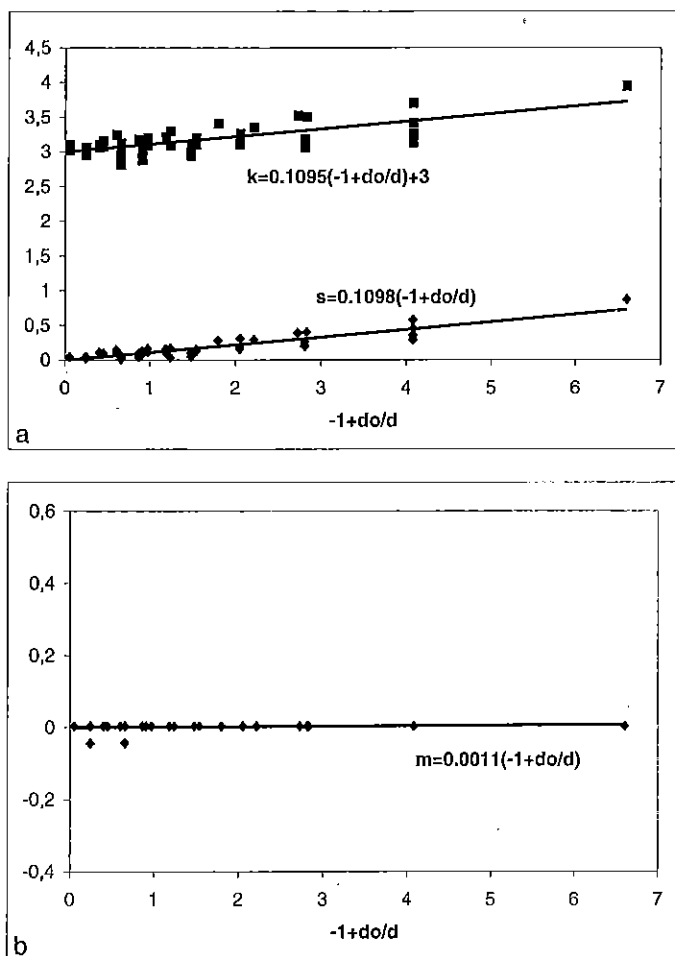


Fig. 9 Variation of  $s$ ,  $k$ ,  $m$  with depth: experimental results

## 6 Conclusions

The discussion presented in this paper along with a set of preliminary results suggest that the short-term probabilistic signature of sea waves can be a viable alternative to spectral description in both deep and shallow waters. Such a representation can provide more information than spectral models and can support the probabilistic design of maritime structures more efficiently than existing procedures.

## Acknowledgments

The valuable help of HR personnel at Wallingford during the experiments, and particularly of R. Whitehouse, A. Channell, R. Soulsby, is gratefully acknowledged. The experimental studies were carried out with financial support from the European Union under the TMR programme for which the authors are thankful. The reviewers of this article should also be thanked for their constructive comments.

## References

1. BITNER, E. M. (1980). Nonlinear effects of the statistical model of shallow-water wind waves. *Appl. Ocean Res.* 2, No. 2, 63-73.
2. CAVANIÉ, A., M. ARHAN, and R. EZRATY (1976). A statistical relationship between individual heights and periods of storm waves. *Proc. Behaviour of Offshore Struct.*, Norwegian Institute of Technology, Trondheim, Norway, 354-360.
3. DALLY, W. R., R. G. DEAN, and R. A. DALRYMPLE (1985). Wave height variation across beaches of arbitrary profile. *J. Geophys. Res.*, 90 (6), 11917-11927.
4. DALLY, W. R. (1992). Random breaking waves: field verification of a wave-by-wave algorithm for engineering application. *Coastal Engrg.*, 16, 369-397.
5. DOERING, J. C., and DONELAN, M. A. (1993). The joint distribution of heights and periods of shoaling waves. *J. Geophys. Res.*, 98(7), 12543-12555.
6. GODA, Y. (1978). The observed joint distribution of periods and heights of ocean waves. *Proc. 16<sup>th</sup> Conf. on Coastal Engrg.*, ASCE, New York, 227-246.
7. GODA, Y. (1986). Effect of wave tilting on zero-crossing wave heights and periods. *Coastal Engrg. in Japan*, Tokyo, 29, 79-90.
8. HOLTHUIJSEN, L. H., N. BOOJI, and R. C. RIS (1993). A spectral wave model for the coastal zone. *Proc. WAVES '93*, ASCE, 630-641.
9. ISHII, T., M. ISOBE, and A. WATANABE (1994). Improved boundary conditions to a time-dependent mild-slope equation for random waves. *Proc. 24<sup>th</sup> Int. Conf. Coastal Engrg.* ASCE, 272-284.
10. KAMPHUIS, J. W. (1994). Wave height from deep water through breaking zone. *J. Wway, Port, Coast. Ocean Div.*, ASCE, 120, No. 4, 347-367.
11. LONGUET-HIGGINS, M. S. (1957). The statistical analysis of a random, moving surface, *Phil. Trans. Roy. Soc. London*, Ser. A (966), 249, 321-387.
12. LONGUET-HIGGINS, M. S. (1963). The effect of non linearities on statistical distributions in the theory of sea waves. *J. Fluid Mech.*, 17, No. 3, 459-480.
13. LONGUET-HIGGINS, M. S. (1983). On the joint distribution of wave periods and amplitudes in a random wave field. *Proc. Royal Soc. London*, 389, 241-258.
14. LOSADA, M. A., and GIMENEZ-CURTO, L. A. (1979). *Coastal Engrg.*, 3, 77-96.
15. MASE, H. (1989). Groupiness factor and wave height distribution. *J. Wway, Port, Coast. Ocean Div.*, ASCE, 115, No. 1, 105-121.
16. MASE, H., and N. KOBAYASHI (1991). Transformation of random breaking waves and its empirical numerical mode considering surf beat. *Proc. Coastal Sediments '91*, ASCE New York, 688-702.
17. MEMOS, C. D. (1994). Experimental results of wave transformation across a sloping beach. *Proc. 24<sup>th</sup> Conf. on Coastal Engrg.*, ASCE, New York, 2350-2364.
18. MEMOS, C. D., and K. TZANIS (1994). Numerical results of the joint probability of heights and periods of sea waves. *Coastal Engrg.*, 22, 217-235.
19. MEMOS, C. D., and K. TZANIS (2000). Joint distribution of wave heights and periods in waters of any depth. *J. Wway Port, Coast. Ocean Engrg.*, ASCE, 126, No. 3, 162-172.
20. MITSUYASU, H. et al. (1975). Observations of the directional spectrum of ocean waves using a cloverleaf buoy. *J. Phys. Oceanogr.*, 5, No. 4, 750-760.
21. NWOGU, O. and E. P. D. MANSARD (1994). Time-domain simulation of directional wave propagation into harbours. *Proc. HYDRO-PORT '94*. Port and Harbour Res. Inst. Yokosuka. 243-265.
22. SIMONS, R., R. J. S. WHITEHOUSE, R. D. MAELVER, J. PEARSON, P. SAYERS, Y. ZHAO, and A. R. CHANNELL (1995). Evaluation of the UK Coastal Research Facility. *Proc. Coastal Dynamics '95*, Gdansk, Poland.
23. STANSBERG, C. T. (1994). Effects from directionality and spectral band-width on nonlinear spatial modulations of deep-water surface gravity wave trans. *Proc. 24<sup>th</sup> Conf. on Coastal Engrg.*, ASCE, New York, 579-593.
24. THORNTON, E. B., and R. T. GUZA (1983). Transformation of wave height distribution. *J. Geophys. Res.*, 88, No. C10, 5925-5938.
25. VAN DER MEER, J. W. (1988). Deterministic and probabilistic design of breakwater armor layers. *J. Wway, Port, Coast. Ocean Engrg.*, ASCE, 114, No. 1, 66-80.
26. WAMDI group: HASSELMANN, S., K. HASSELMANN, E. BAUER, P. A. E. M. JANSSEN, G. J. KOMEN, L. BERTOTTI, P. LIONELLO, A. GUILLAUME, V. C. CARDONE, J. A. GREENWOOD, M. REISTAD, L. ZAMBRESKY, and J. A. EWING (1988). The WAM model - a third generation ocean wave prediction model. *J. Phys. Oceanogr.* 18, 1775-1810.
27. WEGGEL, J. R. (1972). Maximum breaker height. *J. Wway, Harbour, and Coastal Engrg. Div.*, ASCE, 98, No. 4, 529-548.